

Influence of modeling material on undercut slope failure mechanism

M.H. Khosravi^{1*}, T. Pipatpongsa², J. Takemura³ and M. Amini¹

1. School of Mining Engineering, College of Engineering, University of Tehran, Tehran, Iran

2. Construction Engineering Management, Division of Geo-management, Department of Urban Management, Kyoto University, Kyoto, Japan

3. Department of Civil and Environmental Engineering, Tokyo Institute of Technology, Tokyo, Japan

Received 22 April 2017; received in revised form 21 June 2017; accepted 10 July 2017

*Corresponding author: mh.khosravi@ut.ac.ir (M.H. Khosravi).

Abstract

A series of physical modeling tests were conducted by means of a beam type geotechnical centrifuge machine in order to investigate the drainage impact on the slope failure mechanism under centrifugal acceleration. Meanwhile, the phenomenon of stress redistribution in undercut slopes and the formation of arching effect were studied. For this purpose, a poorly graded sandy soil (Silica sand No. 6) as well as a relatively well-graded sandy soil (Edosaki sand) were used as the modeling materials. The humid modeling material was compacted on a low friction oblique rigid plate simulating the potential slippage plane. The process of undercutting was conducted, while the earth pressure redistribution inside the model was recorded by means of a miniature set of pressure cells. The results obtained showed completely different failure mechanisms for the two different modeling soils. By undercutting the slope, the earth pressure redistributed and the arch action was formed in a slope model made from a well-graded soil leading to a clear arch-shaped failure. However, in using the poorly graded soil, the water was drained out during centrifuge g-up, the modeling material properties changed, and an avalanche failure was observed. Therefore, in selecting a humid compacted soil as the centrifugal modeling material, a well-graded soil is recommended.

Keywords: *Centrifugal Modeling, Undercut Slopes, Soil Material Properties, Soil Arching.*

1. Introduction

The existence of a huge and almost flat plane of failure such as a clay seam in a slope can be considered as a critical source of slope instability, especially when it is undercut.

Various techniques have been developed so far to simulate the excavation process for centrifugal modeling. The excavation can be conducted under the 1 g condition with the model mounted in the

centrifuge, and then the driving forces in the model are increased by increasing the centrifugal acceleration until failure occurs [1]. The in-flight excavation can be simulated by replacing the part of the model subjected to the excavation with a rubber bag filled with a heavy liquid under the 1 g condition [2]. Note that the density of the heavy liquid used in this technique should be identical to

that of the soil. The heavy liquid should then be drained out from the model under the target centrifugal acceleration to simulate the in-flight excavation. The advantage of this interesting technique is that the stress equilibrium can be achieved before the test; however, the stress distribution will not be simulated correctly because the liquid cannot sustain a shear stress.

In order to improve the in-flight excavation technique and to properly simulate the excavation process on the centrifuge, an in-flight excavator has been developed in the Tokyo Institute of Technology [3], which consists of a movable table, a cutting blade, and a soil-retaining gate. The movable table sits on a pair of linear rails and can move backwards and forwards. The thrust of the cutting blade is controlled by a stepping motor, which is attached to a pair of screw rods that are connected to the motor using the belt-driven transmission. The vertical movements of the cutting blade are conducted by worm gears built into the stepping motors. In this work, the Mark III beam type of centrifuge machine with the pre-mentioned in-flight excavator, located at the Tokyo Institute of Technology, was used.

The term “undercut slopes” in this work refers to the slopes in open-pit mining, where the excavation process is under operation in front of them. Determination of the optimum undercut span is an important issue in undercut slopes, where, on one hand, this span is limited to a maximum size depending on the strength properties of the slope material and, on the other hand, this span is limited to a minimum size depending on the desired production capacity and the size of the mining equipment.

The existence of some stable scarps in some slope failures in the Mae Moh open-pit Lignite mine of Thailand is an evidence of arch action in those

slopes [4]. Different possible failure mechanisms of undercut slopes were studied through a simple series of 1 g physical models and numerical models [5-8]. Those results were completed later through a series of instrumented physical models and numerical models, where it was confirmed that in calculating the undercut span, the phenomenon of arch action plays an important role [9-18]. This phenomenon in geomaterial has been introduced by Terzaghi [19] as load transferring from a yielding portion of the geomaterial to its stable portions.

Many researchers have carried out studies on soil arch action in different fields, and have investigated this phenomenon theoretically, numerically, and physically [20-26]. The influence of discontinuities such as faults and shear zones has been modeled by means of the 1 g physical modeling [27]. Furthermore, the unstable undercut slopes have been tried to be reinforced by means of different reinforcing techniques such as counterweight balance [28-29] and shear pints [30-32].

The aim of carrying out this research work was to suggest an appropriate modeling material for simulating an undercut slope under centrifugal acceleration and to confirm the formation of arch action in undercut slopes made from an appropriate modeling material.

In this work, a series of centrifugal modelings were conducted under a gravitational acceleration of 50 g.

As the purpose of conducting this work was to study the drainage impact on the failure mechanism of undercut slopes, two different types of granular soils with typical physical and mechanical properties were used under two different excavation techniques. In first technique, each excavation step was conducted under the 1 g

condition, and then the centrifugal acceleration was increased to 50 g. In the second technique, all the excavation steps were conducted under the centrifugal acceleration of 50 g. The behavior of modeling soils are compared and the formation of soil arching is discussed during the following sections.

2. Statement of problem

The existence of a thin oblique clay seam inside the pit wall has been reported by Electrical Generating Authority of Thailand (EGAT) to make some instability problems in the Mae Moh open-pit mine [4, 33]. The problem is illustrated schematically in Figure 1. It was decided to study the mechanism of possible undercut slope failure and formation of arch action through physical modeling. One of the most important parts of a physical modeling is the selection of the material. In order to simulate the mechanism of the problem

correctly, the modeling material should be able to behave similarly to the site material under the same stress conditions.

The previous studies on the Mae Moh open-pit stability problem [4, 34-36] have confirmed that the rock mass on the pit slope in this project is strong enough against failure by itself and the source of instability is the existence of a low resistance clay seam along the pit slope. Compacted humid sand was used as the modeling material, where a low friction Teflon sheet was placed under the compacted sand along the pit slope model. The results of direct shear tests presented in Section 4 confirmed that the interface strength of the compacted soil and Teflon sheet was much lower than the internal strength of the compacted soil. Therefore, it was concluded that the failure mechanism of undercut slopes could be simulated by these materials properly [10, 14, 37].

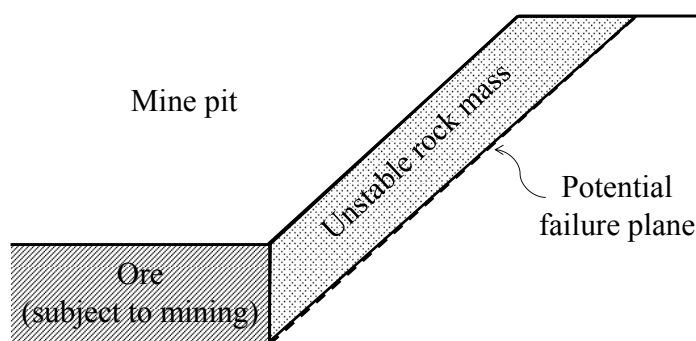


Figure 1. Schematic view of unstable slope.

3. Geotechnical centrifuge machine

The centrifuge used in this work was a beam type of in-house Mark III centrifuge machine, shown schematically in Figure 2. This machine is capable of a maximum payload of up to 1000 kg at an acceleration of 50 g. The physical model should be prepared inside the centrifuge container, and, after instrumentation, the fully assembled package should be uploaded to the platform of the

centrifuge. All the sensors were connected to a data logger located near the axis of the centrifuge, in which the output data could be transmitted through a wireless router to the outside of the centrifuge chamber. On the other hand, the images and video signals from cameras were transmitted through slip rings to the outside of the centrifuge chamber and were monitored during flight.

It is important to note that the centrifugal acceleration varies with the height of the model, which may affect the results. However, this effect is minimized when a centrifuge with a long arm is used [38]. Considering the small height of the

models used in this work (less than 10% of the centrifuge arm), the difference in acceleration, brought about by the height of the model, was ignored, and the acceleration acting on the base of the model was used in the calculation.

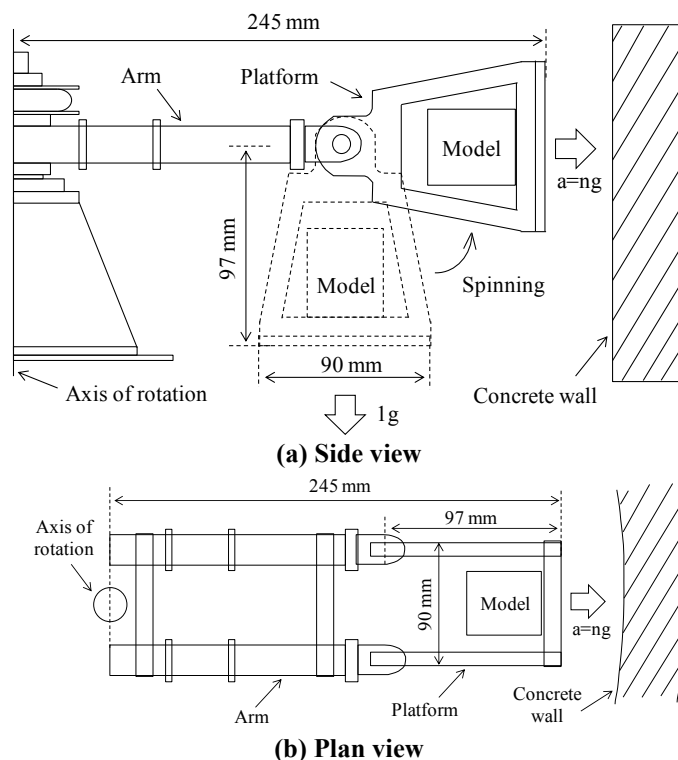


Figure 2. Beam type centrifuge machine used in this work.

4. Modeling material

4.1. Physical properties

Two different types of soil, with an almost equal mean particle size, were investigated in this work as the modeling candidates. The main difference in these soils is their grain size distribution. Silica sand No. 6, a poorly graded soil with a uniformity coefficient of $C_u = 1.42$, was used against Edosaki sand, a relatively well-graded soil with a uniformity coefficient of $C_u = 3.1$. The curves of the grain size distribution for these soils are illustrated in Figure 3.

It is obvious from this figure that the grains of Silica sand No. 6 are more uniform than those of

Edosaki sand. For more clearance, the images obtained using a scanning electron microscope (SEM) for these two types of soil were compared in Figure 4, where the soil textures were enlarged 50 and 200 times. It can be seen that Silica sand No. 6 has very clean angular grains of almost the same size, while Edosaki sand consists of round grains whose voids between the larger grains are filled with smaller grains leading to a lower hydraulic conductivity.

The basic properties of the Silica sand No. 6 and the Edosaki sand used in this work are listed in Table 1.

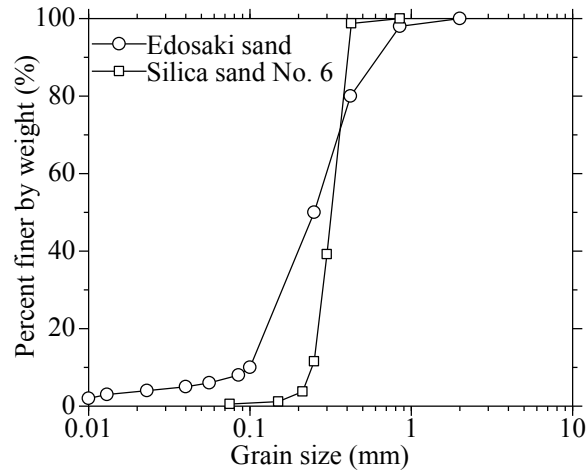
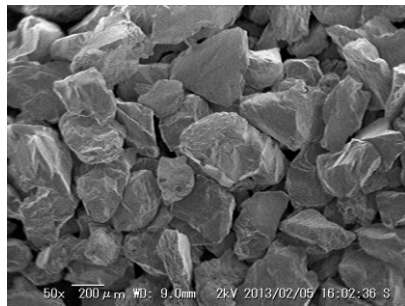
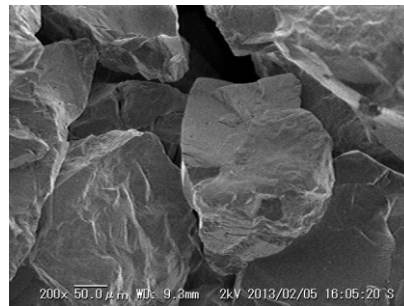


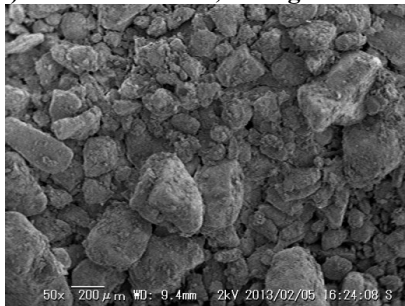
Figure 3. Grain size distribution of Silica sand No. 6 and Edosaki sand.



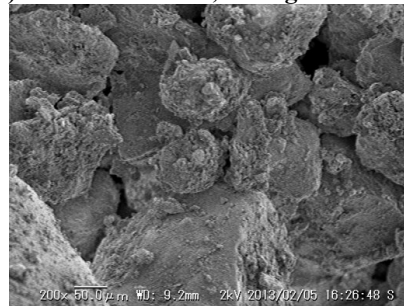
(a) Silica sand No. 6, enlarged 50 times



(b) Silica sand No. 6, enlarged 200 times



(a) Edosaki sand, enlarged 50 times



(b) Edosaki sand, enlarged 200 times

Figure 4. SEM photographs of Silica sand No. 6 and Edosaki sand.

Table 1. Basic properties of humid Silica sand No. 6 and Edosaki sand.

Parameter	Silica sand No. 6	Edosaki sand
Mean particle diameter (D_{50})	0.33 mm	0.25 mm
Uniformity coefficient (C_u)	1.42	3.1
Specific gravity (G_s)	2.65	2.69
Water content (w)	10%	15.4%
Unit weight (γ)	13.7 kN/m ³	16 kN/m ³
Relative density (D_r)	10%	92%
Maximum void ratio (e_{max})	1.132	1.290
Minimum void ratio (e_{min})	0.711	0.870
Cohesion (c)	8 kPa	3.1 kPa
Internal friction angle (ϕ)	41.5°	44.2°

4.2. Shear strength properties

A series of constant-load direct shear tests were conducted on the humid soils compacted and prepared under conditions identical to those of the slope model. The internal friction angle and cohesion of both soils are shown in Table 1.

Teflon was used to simulate the potential failure plane. In order to measure the interface shear strength properties, a direct shear test apparatus was employed. A piece of Teflon plate was cut and fitted in the lower movable part of the shear box, while the upper part of the shear box remained fixed in its position. The soil was prepared inside the upper part of the shear box on the Teflon plate. During the direct shear tests, the soil sample slips on the Teflon plate, and therefore, the interface friction can be measured. The interface friction angles between soil and Teflon were obtained to be 18.5° and 17.5° for Silica sand No. 6 and Edosaki sand, respectively.

4.3. Compatibility of modeling material with instrumentation

The ratio of the pressure cell's effective area to the soil particle size is another important factor involved in the reliability of the physical modeling. For a specified pressure cell with a known effective area, the finer the soil particles, the more accurate the data acquisition for the earth pressure will be. On the other hand, the application of PIV (Particle Image Velocimetry) as an image processing technique requires a material with a sufficient texture for which the image analysis software can reliably detect and identify one image from the next. Therefore, the modeling material should have a particle size to

cover both of the above-mentioned aspects. However, due to the space limitation in the centrifuge modeling container, brought about by the many instruments and the in-flight excavation, image processing was not applied in this work.

The ratio between sensitive cell diameter and mean particle size must be at least 10 [39]. The pressure cells used for this work had a sensitive cell diameter of 6 mm (effective area of 28.3 mm^2), which was quite compatible with both soils employed in the work, considering the mean particle sizes of 0.33 mm and 0.25 mm of Silica sand No. 6 and Edosaki sand, respectively.

5. Experimental set-up

5.1. Model geometry

A slope structure model was created from rigid acrylic plates, as shown in Figure 5. The model consists of a slope part and a toe part. To simulate a potential failure plane in the model, the slope part was covered with a 1 mm-thick Teflon sheet. Furthermore, the toe part was covered with sand paper, simulating a fully rough surface.

Note that it has already been confirmed through direct shear tests that the frictional resistance between the Teflon sheet and the sand is much less than the internal friction of the sand; therefore, it can reliably model a potential failure plane where the failure of the slope will be initiated along it, like a clay seam underlying a sliding layer [4, 40].

The slope structure model was then placed inside a rigid metallic container with a transparent side and the inner dimensions of $493 \text{ mm} \times 300 \text{ mm} \times 360 \text{ mm}$ (length \times width \times height), as shown in Figure 6.

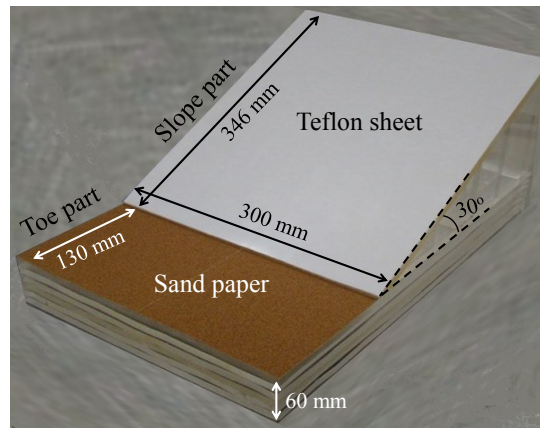


Figure 5. Slope structure model.

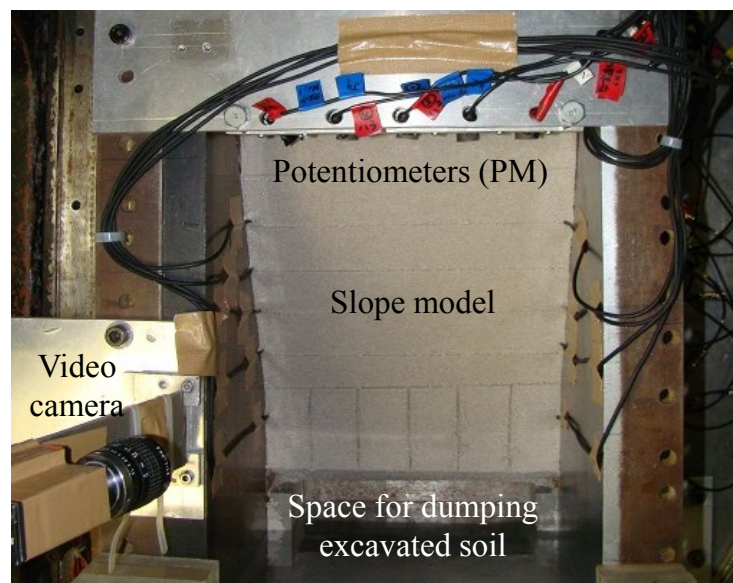


Figure 6. Model prepared in centrifuge container.

5.2. Sample preparation

Moist Silica sand No. 6 (with a water content of 10%) and Edosaki sand (with a water content of 15.4%) were compacted inside the centrifuge model container to achieve the target relative density, as illustrated in Figure 6. A space was provided in front of the model for dumping the excavated soil from the toe part of the model during the in-flight excavation.

5.3. Instrumentation

Pressure cells of type PS-1KC, class ZC were used in this work, where their locations are illustrated in Figure 7. All the pressure cells were

buried 4.5 mm beneath the top layer of sand, with their face orientation either perpendicular to the slope plane or parallel to the side plane of the slope, to measure the earth pressure in the dip direction or the transverse direction.

The pressure values measured by pressure cells P1 and P2 (embedded symmetrically in front of the slope model) are plotted as a function of the centrifugal acceleration in Figure 8.

For both pressure cells, the horizontal pressure measured in the loading stage shows a relatively linear behavior but a non-linear behavior under the unloading stage. This is a typical behavior of diaphragm-based pressure sensors, as reported by

many researchers [41-44]. The reason for the non-linearity behavior of pressure cell during the unloading stage is related to the soil arching around the deflected diaphragm. This type of pressure cells can provide useful data for the purpose of intra-experiment comparison, as in this work, however, their results may not be too accurate to represent the real earth pressure. By applying the principal of ‘null soil pressure system’, hysteresis effects can be significantly reduced or eliminated [43, 45]. However, embedment of such a bulky null pressure cells,

especially in small scale centrifuge models, can lead to a stiff inclusion relative to the soil mass, and reduce the measuring accuracy again.

In order to record the slope movement during the tests, a row of 5 potentiometers of type MLT-38000201, with a range of 60 mm, was installed along the top edge of the slope, as illustrated in Figure 7. Furthermore, a video camera was installed normal to the slope part of the model to monitor the excavation process and to capture the instant of failure. The instrumented model placed on the centrifuge platform is shown in Figure 9.

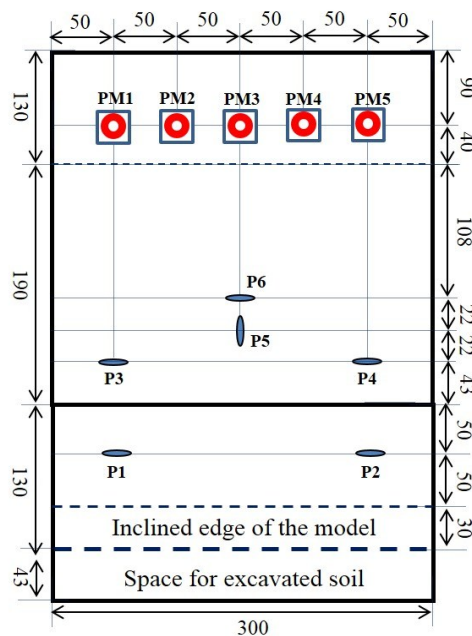


Figure 7. Instrumentation configuration (dimensions in mm).

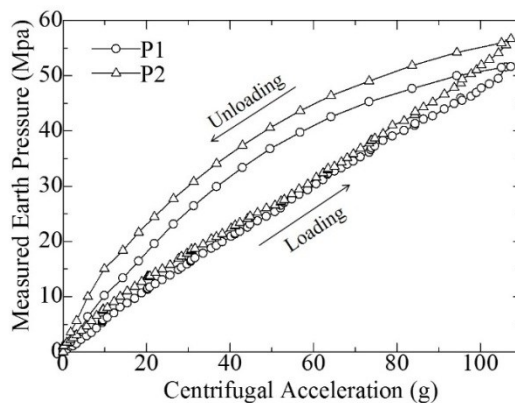


Figure 8. Pressure cell response under one loading-unloading cycle.

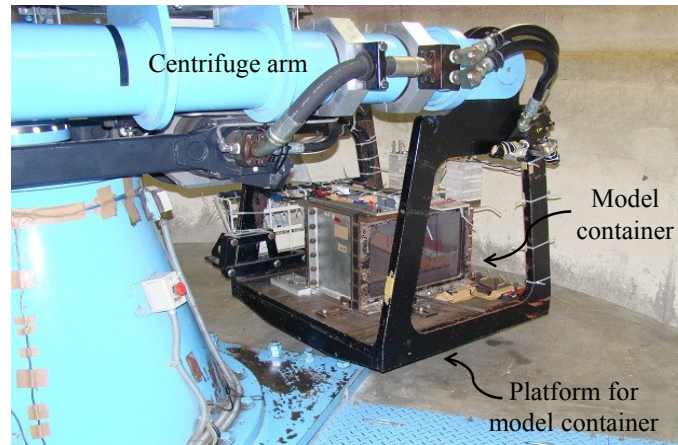


Figure 9. Instrumented model placed on centrifuge platform.

6. Excavation process

Two different excavation techniques were applied to the models in this work. In Test 1, the undercut span excavation was produced under 1 g condition, and then the acceleration was increased to 50 g. In Test 2, the in-flight excavation was experienced at a constant acceleration of 50 g. The excavation processes using these two different techniques are illustrated through a flowchart shown in Figure 10.

The in-flight excavator used in this work was installed on the model container, as shown in Figure 11(a). The excavator consists of a 2D actuator and a cutting blade, where the vertical movement of the cutting blade is controlled by a worm gear built into the stepping motors. The in-flight excavation was conducted at the toe part of the model using the 2D actuator and cutters, as shown schematically in Figure 11(b).

The total span of the excavation was 150 mm, equivalent to 50% of the total width of the model, which was excavated in three steps. The initial excavation step was conducted with a 50 mm-wide cutter at the central portion of the toe. Then the undercut span was expanded to 100 mm during Step 2 of the excavation and to 150 mm during Step 3 symmetrically. The three excavation steps are shown schematically in Figure 12.

The cutters used in this work are shown in Figure 13, where a load cell is placed between the cutter and the holding rod to prevent the cutter's holding rod and the 2D actuator from overloading.

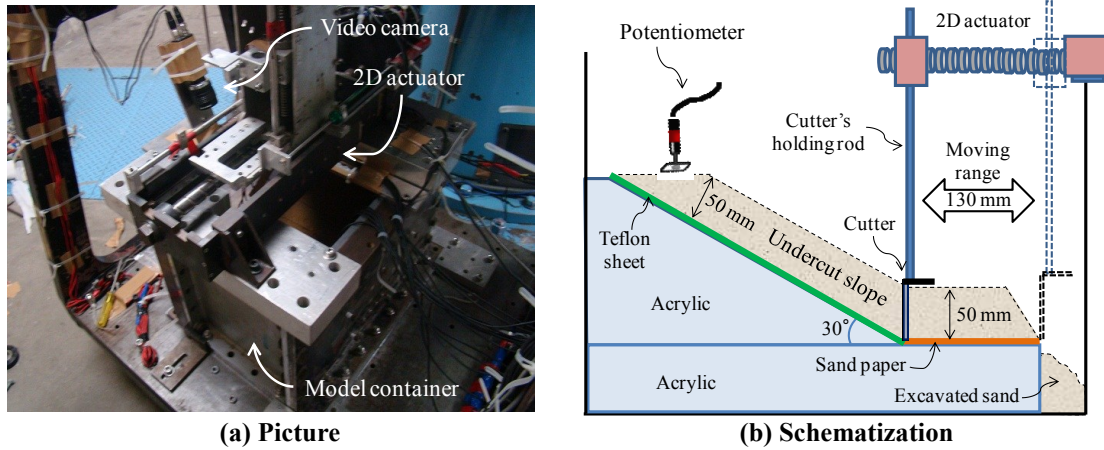
It was confirmed that the two different excavation techniques applied in this work had no effect on the slope failure mechanisms and the difference in failure mechanisms was only due to different material properties.



(a) In-flight excavation

(b) 1-g excavation

Figure 10. Flowchart of two different excavation processes conducted in this work.



(a) Picture
(b) Schematization
Figure 11. In-flight excavator (2D actuator) installed on model container.

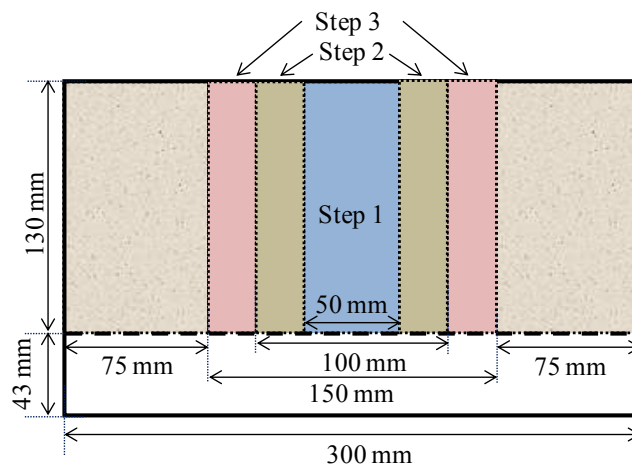
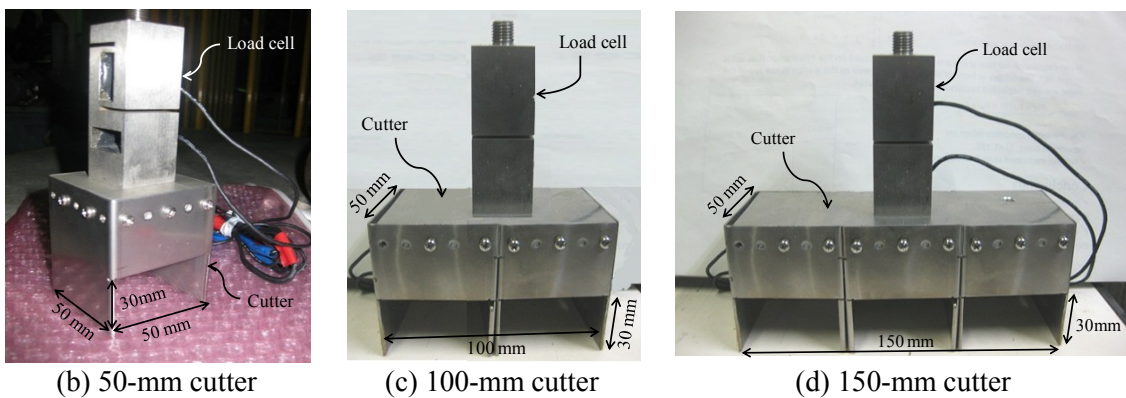


Figure 12. Schematization of excavation steps in front of slope model.



(b) 50-mm cutter
(c) 100-mm cutter
(d) 150-mm cutter
Figure 13. Cutters used for excavation.

7. Experimental results and discussion

7.1. Failure profiles

In the centrifugal modeling, the grain size distribution of the sand is particularly important when unsaturated sand with a specific water content is chosen for use as the modeling material.

When using a poorly graded material such as Silica sand No. 6 (with a uniformity coefficient of $C_u = 1.42$), the increase in the centrifugal acceleration causes the water to drain out of the voids in the soil resulting in a change in the physical and the strength properties of the

material during the tests. It can be seen in Figure 14 that with an increase in the gravitational acceleration, most of the water drained out of the model, leading to an almost 60% decrease in the water content.

On the other hand, when Edosaki sand (with a uniformity coefficient of $C_u = 1$), a well-graded material, is chosen for use as the modeling material, the increase in the gravitational acceleration does not lead to water drainage, which results in a more stable material for the centrifugal modeling.

However, poorly graded materials can be used for the 1 g physical modeling with an acceptable assumption of no drainage during the tests [10, 46].

The slope model made of Silica sand No. 6 gradually lost its original blocky shape due to dewatering by the centrifugal acceleration. This resulted in the drying of the model, especially the top layer, and therefore, dry sand particles flowed in the dip direction even at a very low centrifugal acceleration. The modes of failure for Silica sand No. 6 are shown in Figure 15. For such a model,

the soil block should not be expected to slip on the low resistance interface Teflon plate, despite the very much lower interface friction compared to the higher shear strength properties of the soil. Instead, the model of slope failure was an avalanche of dewatered sand particles.

On the other hand, the slope model made of Edosaki sand showed a stable appearance. As illustrated in Figure 16, the soil block in this model maintained its blocky shape throughout the test, and failure occurred due to soil slippage on the Teflon plate. By increasing the undercut span, a larger arched-shaped area slipped until the total slip of the slope block occurred when the remaining toes were weak enough to buckle under the high pressure transferred to them by the arch action [47].

At the Mae Moh open-pit mine, the unstable rock mass is strong enough by itself, and the source of instability is the weak clay seam underlying it [4, 48], therefore, the expected mode of failure is what occurred in model test 2, using Edosaki sand.



Figure 14. Water drainage from Silica sand. No. 6 model during g-up process.

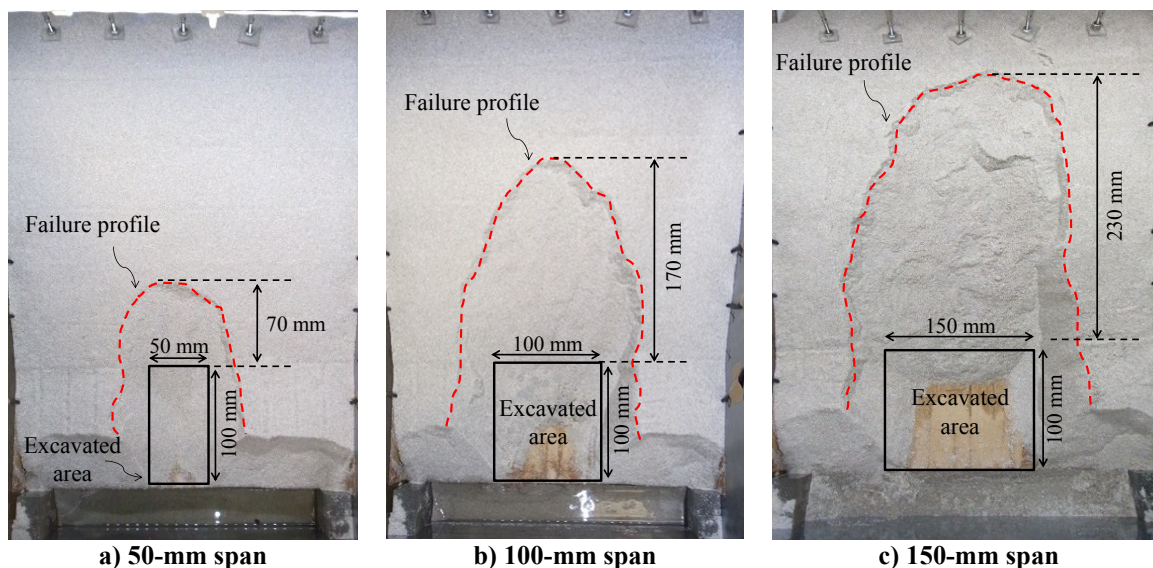


Figure 15. Failure modes in Silica sand No. 6 model.

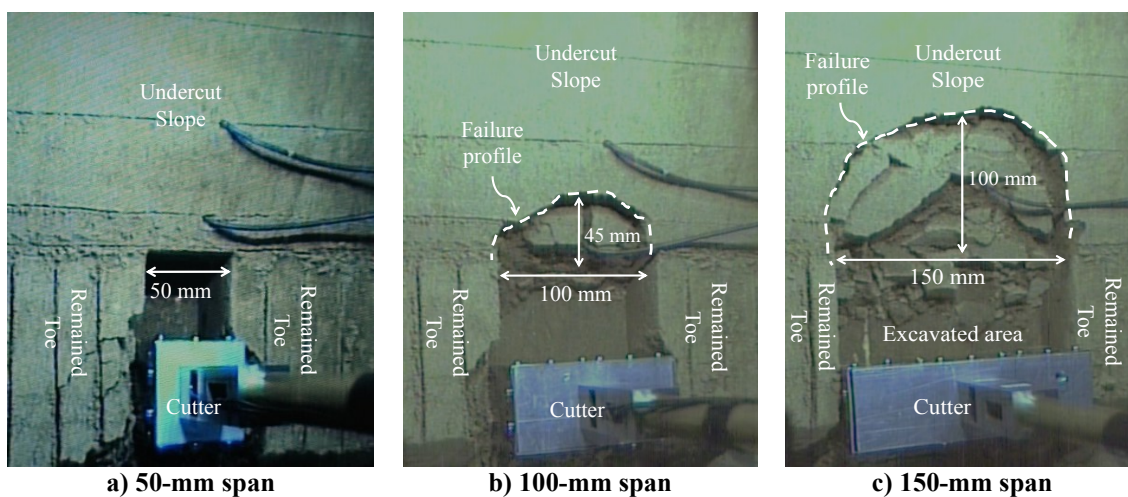


Figure 16. Failure modes in Edosaki sand model.

7.2. Earth pressure redistribution

The changes in earth pressure with time for the slope model made of Edosaki sand are shown in Figure 17.

The pressure cells at the toe part of the model (P1 and P2) represent almost no change in pressure during the excavation, except for the last step, when general slope slippage occurred. The pressure cells at the sides of the slope (P3 and P4) represent a steady increase in earth pressure during the excavation, while the pressure cell at the central part of the slope (P6) represents a steady decrease in the earth pressure. This phenomenon can be explained by the arching

effect, when the load transfers from the yielding central part to the adjacent stationary parts of the model. Furthermore, at the central part of the slope, the state of stress is initially in an active condition, where the pressure in the dip direction (P6) is higher than that in the transverse direction (P5). The excavation leads to an increase in P5 and a decrease in P6 until P5 reaches P6 at a certain time. Therefore, the state of stress tends to switch from active to passive. These results are consistent with the results of 1 g undercut slope model tests [10]. As the excavation span is increased to 150 mm (step 3), the soil around pressure cell P5 fails and P5 data is reduced to

zero. Furthermore, pressure cell P3 shows a sudden decrease indicating the movement of the left side of the model. Finally, at the end of excavation, step 3, the soil around pressure cell P6 failed and P6 data is also reduced to zero (see Figure 17).

For the model made of Silica sand No. 6, the undercut span was prepared under the 1 g

condition and the centrifugal acceleration was increased to 50 g. This process was repeated for three different undercut spans of 5 cm, 10 cm, and 15 cm. The earth pressure recorded by the pressure cells, during the g-up and g-down processes, is shown in Figure 18.

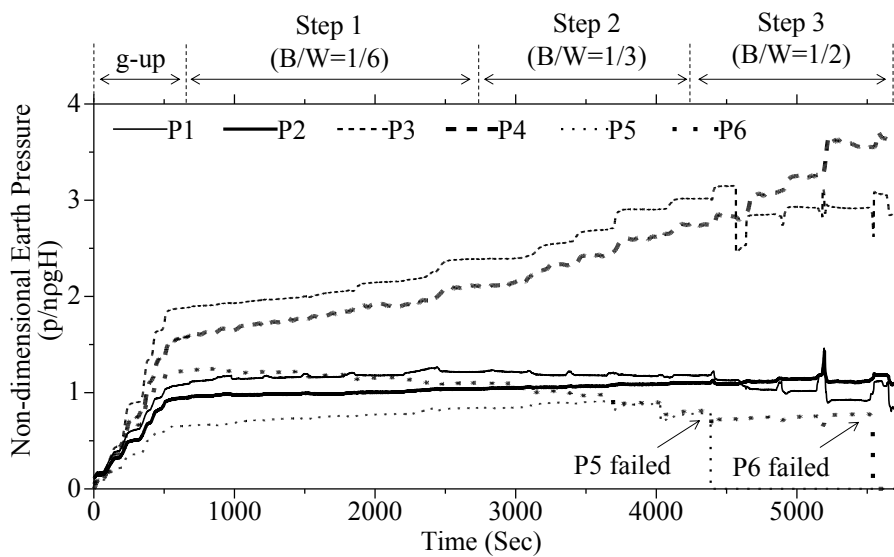


Figure 17. Measured earth pressure vs. time for slope model made of Edosaki sand (B and W represent undercut span and model width, respectively).

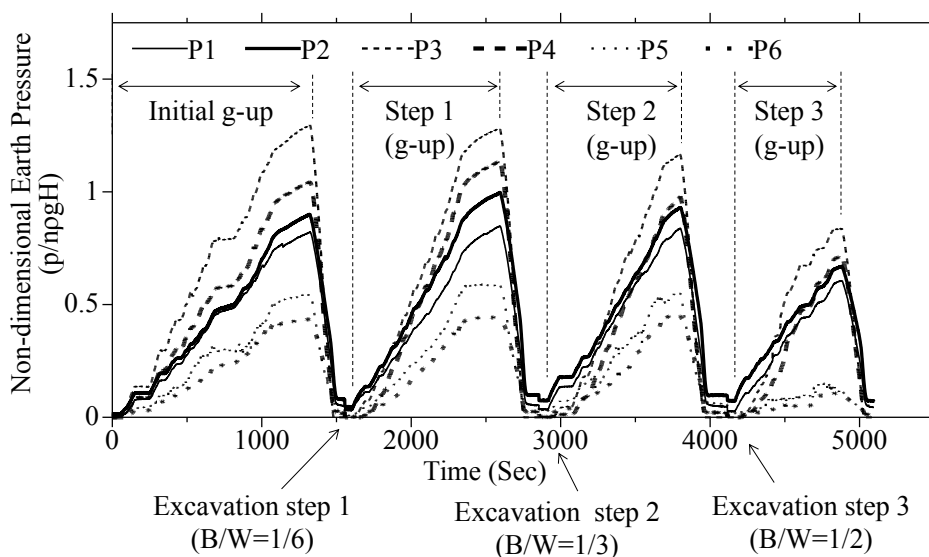


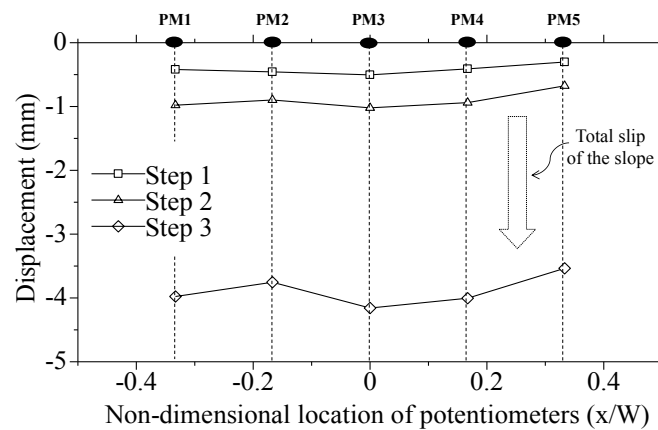
Figure 18. Measured earth pressure vs. time for slope model made of Silica sand No. 6 (B and W represent undercut span and model width, respectively).

Due to the water leakage in this model, the soil dried out, which brought about some settlement. The soil settlement resulted in the passive earth pressure condition even before any excavation was conducted in the model. The evidence of this phenomenon is that the recording of P5 (the pressure cell measuring the earth pressure in the transverse direction) is more than P6 (the pressure cell measuring the earth pressure in the dip direction). For the other pressure cells (P1 to P4), the earth pressure decreases for every excavation step. This is inconsistent with the results of the model made of Edosaki sand, and therefore, with the arching effect. The reason is that when the soil is dried out, the model loses its original blocky shape, cannot sustain high shear stress, and therefore, cannot transfer the load from the

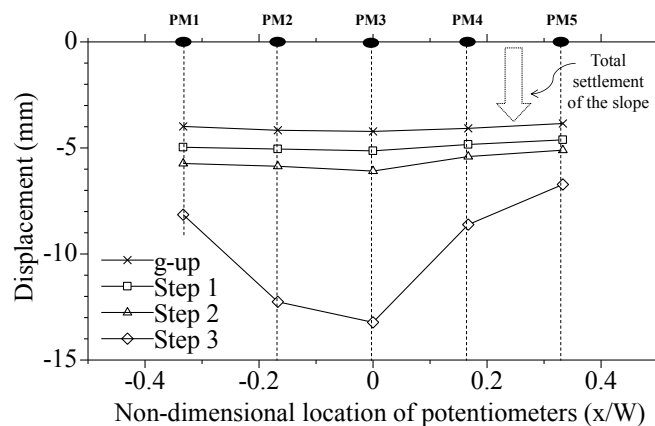
yielding central part to the adjacent stationary parts.

7.3. Slope displacement

The slope deformation during the excavation process is shown in Figure 19. In the model made of Edosaki sand, the slope displacement during Steps 1 and 2 of the excavation is uniform with a total displacement of less than 1 mm. In the middle of Step 3 of the excavation, a total slip of 3 mm is observed (Figure 19(a)). On the other hand, in the model made of Silica sand No. 6, a total settlement of 4 mm was observed during the g-up process (Figure 19(b)). As mentioned earlier, this settlement is due to the water drainage at the high centrifugal acceleration.



(a) Slope model made of Edosaki sand.



(b) Slope model made of Silica sand No. 6.

Figure 19. Profile of slope top after Step 3 of excavation.

8. Conclusions

Two different types of sand were used for the centrifugal modeling of undercut slopes, Silica sand No. 6, a poorly graded soil, and Edosaki sand, a relatively well-graded soil. The purpose was to study the drainage impact on the failure mechanism of an undercut slope, where a potential slippage plane is the source of instability. The humid soil was compacted on a Teflon plate simulating a potential slippage plane. It was observed that with increase in the centrifugal acceleration, the poorly graded sand was not able to sustain its original water content. Therefore, the water was drained out of the model, leading to a change in the soil's strength properties, and the slope failed in an avalanche form. On the other hand, the relatively well-graded Edosaki sand was able to sustain its original water content even at the high centrifugal acceleration of 50 g, and a clear arch-shaped slope failure was observed. For the centrifugal modeling, in the case of a humid soil, a well-graded soil is recommended in order to minimize the changes in material strength due to the water drainage during the centrifugal acceleration. Studying the behavior of undercut slopes under centrifugal modeling is a new subject of research, which has recently been pioneered by the Tokyo Institute of Technology. Of course, much more investigations such as physical modeling under dynamic conditions and numerical modeling is required to improve our understanding on the behavior of these types of slopes.

Acknowledgments

This work was supported financially by the Global COE Program, Center for Urban Earthquake Engineering (CUEE). The helpful

assistance of Mr. Sakae Seki during the performance of the centrifugal model tests is appreciated. Also we would like to express our gratitude to EGAT (Electricity Generating Authority of Thailand) for providing the research data of the mining site.

Notation

The following symbols are used in this paper:

- B = undercut span
- C_u = uniformity coefficient
- c, c_i = cohesion and interface adhesion, respectively
- D_{50} = Mean particle diameter
- D_r = relative density
- e_{max}, e_{min} = maximum and minimum void ratio, respectively
- G_s = specific gravity
- g, ng = gravitational and centrifugal acceleration, respectively
- H = height of the soil in the model
- W = model width
- w = water content
- γ = bulk unit weight of the soil
- ρ = bulk density of the soil in the model
- σ_c = unconfined compressive strength of the soil
- ϕ, ϕ_i = internal and interface friction angles, respectively

References

- [1]. Lyndon, A. and Schofield, A.N. (1970). Centrifuge model test of short term failure in London clay. *Geotechnique*. 20 (4): 440-442.
- [2]. Kusakabe, O. (1982). Stability of excavation in soft clay. Cambridge University. PhD dissertation.
- [3]. Takemura, J., Kondoh, M., Esaki, T., Kouda, M. and Kusakabe, O. (1999). Centrifuge model tests on

double propped wall excavation in soft clay. *Soils and Foundations*. 39 (3): 75-87.

[4]. Pipatpongsa, T., Khosravi, M.H., Doncommul, P. and Mavong, N. (2009). Excavation problems in Mae Moh lignite open-pit mine of Thailand. *Proceedings of Geo-Kanto conference*. Tohigi. pp. 459-464.

[5]. Khosravi, M.H., Pipatpongsa, T., Leelasukseree, C. and Wattanachai, P. (2009). Failure mechanisms in arched excavation of sloped earth using model test, *Proceedings of Geo-Kanto 2009*, pp. 241-246.

[6]. Pipatpongsa, T., Khosravi, M.H., Leelasukseree, C., Mavong, N. and Takemura, J. (2010). Slope failures along oblique plane due to sequential removals of propping portion in physical model tests. *The 15th National Convention on Civil Engineering of Thailand*.

[7]. Leelasukseree, C., Khosravi, M.H., Pipatpongsa, T. and Mavong, N. (2010). Investigation of load transfer mechanisms due to undercutting at toe of slope resting on sliding plane by using 3D elastic analyses. *The 12th International Summer Symposium*. pp. 195-198.

[8]. Pipatpongsa, T., Leelasukseree, C., Khosravi, M.H. and Mavong, N. (2010). Arch action in granular media placing along an oblique plane across an undercut pit examined by computer simulations. *JSCE Annual Meeting*. pp. 783-784.

[9]. Khosravi, M.H., Ishii, Y., Takemura, J. and Pipatpongsa, T. (2010). Centrifuge model test on compacted sand slopes undercut by in-flight excavator. *The Japanese Geotechnical Society, Geo-Kanto 2010*. pp. 136-139.

[10]. Khosravi, M.H., Pipatpongsa, T., Takahashi, A. and Takemura, J. (2011). Arch action over an excavated pit on a stable scarp investigated by physical model tests. *Soils and Foundations*. 51 (4): 723-735.

[11]. Pipatpongsa, T., Khosravi, M.H., Stathas, D., Leelasukseree, C. and Takemura, J. (2012). Cohesive

arch action in laterally confined block of moist sand placing on an inclined bedding plane. *ISRM Regional Symposium- 7th Asian Rock Mechanics Symposium*.

[12]. Leelasukseree, C., Pipatpongsa, T., Khosravi, M.H. and Mavong, N. (2012). Stresses and a failure mode from physical and numerical models of undercut slope lying on inclined bedding plane. *The 7th Asian Rock Mechanics Symposium*. Seoul. Korea.

[13]. Pipatpongsa, T., Khosravi, M.H., Stathas, D. and Takemura, J. (2012). Effect evaluation of tensile strength to a critical width of undercut slope aligned with a bedding plane. *The 47th Japan National Conference on Geotechnical Engineering*. pp. 777-778.

[14]. Khosravi, M.H., Pipatpongsa, T. and Takemura, J. (2012). Pseudo-static analysis of passive arch action in undercut slopes against earthquake. *Proceedings of the 9th International Conference on Urban Earthquake Engineering*. Tokyo. pp. 665-672.

[15]. Techawongsakorn, T., Hirai, H., Khosravi, M.H. and Pipatpongsa, T. (2013). Slip mechanisms and interface shear strength between moist silica sand and acrylic plate. *The 48th Japan National Conference on Geotechnical Engineering*. pp. 895-896.

[16]. Hirai, H., Khosravi, M.H. and Pipatpongsa, T. (2013). Geometrical shape of arch formed by collapse of undercut slope. *The 62nd National Congress of Theoretical and Applied Mechanics Japan*. pp. 13-04.

[17]. Pipatpongsa, T., Khosravi, M.H. and Takemura, J. (2013). Physical modeling of arch action in undercut slopes with actual engineering practice to Mae Moh open-pit mine of Thailand. *Proceedings of the 18th International Conference on Soil Mechanics and Geotechnical Engineering (ICSMGE18)*. Paris. France. pp. 943-946.

[18]. Khosravi, M.H., Takemura, J. and Pipatpongsa, T. (2013). Centrifugal modeling of undercut slopes

subjected to pseudo-static loading. The 10th International Conference on Urban Earthquake Engineering, pp. 523-532.

[19]. Terzaghi, K. (1936). Stress distribution in dry and saturated sand above a yielding trap-door. Proceedings of the 1st International Conference on Soil Mechanics and Foundation Engineering. Harvard University. Cambridge. pp. 307-311.

[20]. Spangler, M.G. (1964). Protection of underground structures by arch action associated with the imperfect ditch method of construction. Proceedings of the Symposium on Soil-Structure Interaction. University of Arizona. Tucson. Arizona. pp. 531-546.

[21]. Getzler, Z., Komornik, A. and Mazurik, A. (1968). Model study on arching above buried structures. Journal of Soil Mechanics and Foundation Division. ASCE 94 (SM5): 1123-1141.

[22]. Handy, R.L. (1985). The Arch in soil arching. Journal of Geotechnical Engineering. ASCE 111 (3): 302-318.

[23]. Bosscher, J. and Gray, H. (1986). Soil arching in sandy slopes. Journal of Geotechnical Engineering. ASCE 112 (6): 626-645.

[24]. Khosravi, M.H., Pipatpongsa, T. and Takemura, J. (2013). Experimental analysis of earth pressure against rigid retaining walls under translation mode. Geotechnique. 63 (12): 1020-1028.

[25]. Ashour, M. and Ardalan, H. (2012). Analysis of pile stabilized slopes based on soil- pile interaction. Computers and Geotechnics. 39: 85-97.

[26]. He, Y., Hazarika, H., Yasufuku, N. and Han, Z. (2015). Evaluating the effect of slope angle on the distribution of the soil-pile pressure acting on stabilizing piles in sandy slopes. Computers and Geotechnics. 69: 153-165.

[27]. Techawongsakorn, T., Pipatpongsa, T., Khosravi, M.H. and Borely, C. (2013). Failure mechanism of undercut slope with planes of discontinuity. The 5th Multidisciplinary International Student Workshop.

[28]. Khosravi, M.H., Tang, L., Pipatpongsa, T., Takemura, J. and Doncommul, P. (2012). Performance of counterweight balance on stability of undercut slope evaluated by physical modeling. International Journal of Geotechnical Engineering. 6 (2): 193-205.

[29]. Khosravi, M.H., Sarfaraz, H., Esmailvandi, M. and Pipatpongsa, T. (2017). A Numerical Analysis on the Performance of Counterweight Balance on the Stability of Undercut Slopes. Int. Journal of Mining & Geo-Engineering. 51 (1): 63-69.

[30]. Ouch, R., Ukritchon, B., Pipatpongsa, T. and Khosravi, M.H. (2016). Experimental investigations of shear pin arrangement on soil slope resting on low interface friction plane. Maejo International Journal of Science and Technology, 10 (03): 313-329.

[31]. Ukritchon, B., Ouch, R., Pipatpongsa, T. and Khosravi, M.H. (2017). Experimental studies of floor slip tests on soil blocks reinforced by brittle shear pins, International Journal of Geotechnical Engineering, Published online. <http://dx.doi.org/10.1080/19386362.2017.1314126>.

[32]. Ouch, R., Ukritchon, B., Pipatpongsa, T. and Khosravi, M.H. (2017). Finite element analyses of the stability of a soil block reinforced by shear pins. Geomechanics and Engineering. Published online. <https://doi.org/10.12989/gae.2017.12.6.000>.

[33]. EGAT. (1985). Thailand-Australia Lignite Mines Development Project. Geotechnical Report for Mae Moh Mine. Vol 3.

[34]. Khosravi, M.H., Pipatpongsa, T., Takemura, J., Mavong, N. and Doncommul, P. (2011). Investigation on shear strength of shale at the Mae Moh open-pit

mine. The 4th Thailand-Japan International Academic Conference. pp. 51-52.

[35]. Khosravi, M.H., Pipatpongsa, T., Takemura, J. and Doncommul, P. (2011). Alternative coal mining method with lesser energy and environmental load The Asia-Oceania Top University League on Engineering (AOTULE 2011). Beijing. China.

[36]. Khosravi, M.H., Pipatpongsa, T., Takemura, J. and Doncommul, P. (2012). Investigation on strength properties of lignite at the Mae-Moh open-pit mine. The 5th Thailand-Japan International Academic Conference 2012.

[37]. Khosravi, M.H., Pipatpongsa, T. and Takemura, J. (2013). Interface shearing resistance properties between moist silica sand and surface of materials investigated by direct shear apparatus. The Japanese Geotechnical Society, Geo-Kanto.

[38]. Ling, H.I., Wu, M., Leshchinsky, D. and Leshchinsky, B. (2009). Centrifuge modeling of slope instability. *Journal of Geotechnical and Geoenvironmental Engineering*. 135 (6): 758-767.

[39]. Weiler, W.A. and Kulhawy, F.H. (1982). Factors affecting stress cell measurements in soil. *Journal of the Geotechnical and Foundation Division*. ASCE 108 (GT12): 1529-1548.

[40]. Ohta, H., Pipatpongsa, T., Heng, S., Yokota, S. and Takemoto, M. (2010). Significance of saturated clays seams for the stability of rainfall-induced landslides. *Bulletin of Engineering Geology and the Environment*. 69 (1): 71-87.

[41]. Clayton, C.R.I. and Bica, A.V.D. (1993). The design of diaphragm-type boundary total stress cells. *Geotechnique*. 43 (4): 523-535.

[42]. Miura, K., Otsuka, N., Kohama, E., Supachawarote, C. and Hirabayashi, T. (2003). The size effects of earth pressure cells on measurement in granular materials. *Soils and Foundations*. 43 (5): 133-147.

[43]. Talesnick, M. (2005). Measuring soil contact pressure on a solid boundary and quantifying soil arching. *ASTM Journal of Geotechnical Testing*. 28 (2): 171-179.

[44]. Arshad, M. and O'Kelly, B.C. (2014). Use of Miniature Soil Stress Measuring Cells under Repeating Loads. *Information Technology in Geo-Engineering*. doi:10.3233/978-1-61499-417-6-177.

[45]. Li, U., Talesnick, M.L. and Bolton, M. (2014). Use of null gauges to monitor soil stresses during excavation in a centrifuge. *International Journal of Physical Modelling in Geotechnics*. 14 (2): 40-53.

[46]. Khosravi, M.H. (2012). Arching effect in geomaterials with applications to retaining walls and undercut slopes. Department of International Development Engineering. Graduate School of Science and Engineering. Tokyo Institute of Technology. PhD dissertation.

[47]. Khosravi, M.H., Takemura, J., Pipatpongsa, T. and Amini, M. (2016). In-flight excavation of slopes with potential failure planes. *Journal of Geotechnical and Geoenvironmental Engineering*. 142 (5): 06016001.

[48]. Pipatpongsa, T., Khosravi, M.H., Takemura, J. and Leelasukseree, C. (2016). Modelling concepts of passive arch action in undercut slopes. *The First Asia Pacific Slope Stability in Mining Conference*. Perth. Australia.

بررسی تأثیر نوع مواد در مکانیسم شکست شیروانی‌های تحت حفاری

محمد حسین خسروی^{۱*}، تیراپونگ پیپاتپونگسا^۲، جیرو تاکمورا^۳ و مهدی امینی^۱

۱- دانشکده مهندسی معدن، پردیس دانشکده‌های فنی، دانشگاه تهران، ایران

۲- دپارتمان مدیریت شهری، پردیس کانسورا، دانشگاه کیوتو، ژاپن

۳- دپارتمان مهندسی عمران و محیط‌زیست، انستیتو فناوری توکیو، ژاپن

ارسال ۲۰۱۷/۴/۲۲، پذیرش ۲۰۱۷/۷/۱۰

* نویسنده مسئول مکاتبات: mh.khosravi@ut.ac.ir

چکیده:

به منظور مطالعه تأثیر نوع مواد دانه‌ای بر مکانیسم شکست شیروانی‌ها در مدل‌سازی تحت شتاب دورانی بالا، یک سری آزمایش مدل‌سازی فیزیکی با استفاده از یک ماشین سانتریفیوژ ژئوتکنیکی انجام شده است. در این آزمایش‌ها پدیده توزیع مجدد تنش‌ها در شیروانی تحت حفاری و ساختار قوس‌زدگی نیز مطالعه شده است. برای این هدف از دو نوع متفاوت خاک دانه‌ای یعنی خاک با دانه‌بندی خوب (ماسه ادوساکی) و خاک با دانه‌بندی ضعیف (ماسه سیلیکای شماره ۶)، به عنوان مواد مدل‌سازی استفاده شده است. خاک دانه‌ای مورد نظر به صورت مرطوب بر روی یک صفحه صلب کم اصطکاک به عنوان صفحه با پتانسیل لغزش متراکم شده است. فرآیند زیربرش در مدل انجام شده در حالی که توزیع تنش‌ها در مدل به وسیله یک سری فشارسنج مینیاتوری ثبت می‌شود، انجام شد. نتایج این مدل‌سازی، مکانیسم‌های شکست کاملاً متفاوتی را برای دو نوع خاک مورد استفاده نشان داد. در مدل ساخته شده با خاک با دانه‌بندی خوب، با ایجاد زیربرش و افزایش شتاب دورانی، مدل قادر به حفظ خصوصیات مقاومتی بوده و توزیع مجدد تنش‌ها حاکی از شکل‌گیری قوس فشارسنج مینیاتوری ثبت می‌شود، انجام شد. نتایج این مدل‌سازی، مکانیسم‌های شکست کاملاً متفاوتی را برای دو نوع خاک مورد استفاده نشان داد. در مدل ساخته شده با خاک با دانه‌بندی خوب، با ایجاد زیربرش و افزایش شتاب دورانی، مدل قادر به حفظ خصوصیات مقاومتی بوده و توزیع مجدد تنش‌ها حاکی از شکل‌گیری قوس فشارسنج مینیاتوری ثبت می‌شود، انجام شد. نتایج این مدل‌سازی، مکانیسم‌های شکست کاملاً متفاوتی را برای دو نوع خاک مورد استفاده نشان داد. در مدل ساخته شده با خاک با دانه‌بندی ضعیف، با افزایش شتاب دورانی سانتریفیوژ بخشی از آب موجود در بین دانه‌های خاک در بیرون زهکش شده و منجر به تغییر در خصوصیات مقاومتی مدل شده و در نتیجه شکست شیروانی به صورت ریزشی و بهمین اتفاق افتاد؛ بنابراین در مواردی از مدل‌سازی فیزیکی با استفاده از سانتریفیوژ ژئوتکنیکی که قرار است از خاک دانه‌ای متراکم با یک درصد رطوبت خاص به عنوان مواد مدل‌سازی استفاده شود، توصیه می‌شود که از خاک با دانه‌بندی خوب استفاده شود.

کلمات کلیدی: مدل‌سازی با سانتریفیوژ، شیروانی تحت حفاری، خصوصیات خاک مدل‌سازی، قوس زدگی.